Journal of Molecular Liquids 313 (2020) 113490

Contents lists available at ScienceDirect

Journal of Molecular Liquids

journal homepage: www.elsevier.com/locate/molliq

Molecular interactions of ceftazidime with bovine serum albumin: Spectroscopic, molecular docking, and DFT analyses

Mohd. Sajid Ali [a,*], Jayaraman Muthukumaran [b], Hamad A. Al-Lohedan [a]

[a] Surfactant Research Chair, Department of Chemistry, College of Science, King Saud University, P.O. Box-2455, Riyadh 11451, Saudi Arabia
[b] Department of Biotechnology, School of Engineering and Technology, Sharda University, P.C. 201 310, Greater Noida, U.P., India

ARTICLE INFO

Article history:
Received 11 December 2019
Received in revised form 23 May 2020
Accepted 30 May 2020
Available online 02 June 2020

Keywords:
Ceftazidime
Bovine serum albumin
Fluorescence
Inner filter effect
DFT
Molecular docking

ABSTRACT

Ceftazidime is a well-known cephalosporin antibiotic included in the World Health Organization's list of essential medicines. Herein, we investigated the molecular interactions of ceftazidime with bovine serum albumin (BSA) using detailed steady-state fluorescence spectroscopy supported by ultraviolet–visible and circular dichroism spectroscopies together with comprehensive molecular docking and density functional theory analyses. The formation of complex between ceftazidime and BSA was confirmed by the changes observed in the electronic spectra of BSA in the absence and presence of the drug. In particular, ceftazidime quenched the fluorescence emission of BSA and the inner filter effect was also corrected before the data analysis, as it significantly affected the fluorescence quenching. Moreover, the static quenching mechanism was proved to be involved in the 1:1 binding between BSA and ceftazidime, and ceftazidime partially unfolded the protein. Based on the experimental data, the interaction was mainly due to hydrophobic interactions, and molecular docking analysis revealed that other forces, such as hydrogen bonding and van der Waals, were also involved in the interaction. The primary binding site of ceftazidime in BSA was the interfacial region of the three domains with the maximum participation of domain 1. Frontier molecular orbital calculations demonstrated that the complexed ceftazidime was more stable than the free state, implying the formation of a stable complex with BSA, which was also consistent with the spontaneity of the experimentally identified interactions.

1. Introduction

Antibiotics are considered as one of the best chemotherapeutic agents [1], as they can be used to control various life-threatening infections, especially diseases caused by bacteria. To date, a wide range of antibiotics has been discovered based on the very first systematic investigations and discoveries by Ehrlich and Fleming [2,3]. Cephalosporins, a large group of broad-spectrum antibiotics, belong to the class of β-lactam antibiotics initially obtained from the fungus *Acremonium*, which is also known as *Cephalosporium*, while their structure and antimicrobial activity are similar to those of penicillin [4].

Ceftazidime is a third-generation cephalosporin antibiotic, included in the World Health Organization's (WHO) list of essential medicines, which comprises the most effective and safe medicines for the health system [5]. Although ceftazidime has not been approved by the Food and Drug Administration (FDA) for use in animals, it has been used for the treatment of certain animal infections [6]. Ceftazidime can be administered intravenously or intramuscularly and has relatively less side effects compared to other antibiotics and no routine drug plasma concentration monitoring is required [7]. Moreover, in contrast to other third-generation cephalosporins [8], it exhibits significant clinical activity to *Pseudomonas aeruginosa*, a Gram negative bacterium responsible for severe acute and chronic infections [9]. Ceftazidime is also resistant to hydrolysis by most β-lactamases, enzymes produced by bacteria providing multi-resistance to β-lactam antibiotics. According to a detailed review of Richards and Brogden, the peak ceftazidime serum concentrations (70–72 mg/L) are immediately achieved after the infusion of 1 g, administered over a period of 20–60 min. Its elimination half-life in healthy subjects has been found to be 1.5–2.8 h, as the drug is not metabolized and a large amount is eliminated via the urine. In addition, it has been reported that the therapeutic concentrations of ceftazidime can be achieved in various tissues and body fluids such as female genital tissue, bones, peritoneal, extravascular, lymphatic, amniotic fluid, etc. [7].

When a drug is administered to the body, irrespective of the administration method, it is usually bound to plasma proteins, especially serum albumins, which are the main binders and carriers of drugs throughout the body [10]. Serum albumins are large globular proteins with a molecular mass of around 66 kDa. In addition to exogenous substances, they can also bind to several endogenous substances such as fatty acids and bilirubin. Bovine serum albumin (BSA) is one of the

* Corresponding author.
E-mail addresses: smsajidali@gmail.com, msali@ksu.edu.sa (M.S. Ali).

https://doi.org/10.1016/j.molliq.2020.113490
0167-7322/

most studied proteins and, due to its 76% structural homology with its human counterparts [11], it is used as a standard model to understand the binding mechanism of carrier proteins with drugs. Given that the in vivo non-covalent interactions between biomolecules and therapeutic agents are complicated due to the complex nature of the biological systems, in vitro studies are usually applied, providing significant information on specific interactions between biomolecules and small molecules and their binding mechanism and effectiveness [12–15].

In this study, we investigated the binding of ceftazidime to BSA due to the excellent therapeutic value of ceftazidime for humans and animals and the suitability of BSA as a model system for understanding the drug binding mechanism. Although the binding of serum albumins with ceftazidime has been previously reported [16–18], the correction of the inner filter effect has not been considered. Earlier studies revealed that the inner filter effect can significantly affect the fluorescence quenching of proteins, if the quencher has a strong absorption at the excitation and emission wavelengths of the protein. Therefore, ignoring the inner filter effect correction may lead to invalid results [19–21]. To that end, this study aims to elucidate the binding mechanism after correcting the inner filter effect. Furthermore, a detailed molecular docking study was performed to identify the most preferred binding site of ceftazidime within BSA.

2. Materials and methods

BSA (≥98%, A7030) and ceftazidime (≥90%, C3809) were purchased from Sigma. The studies were carried out in 20 mM Tris-HCl buffer (pH 7.4). The ultraviolet–visible (UV–Vis) spectra were obtained by a Perkin Elmer Lambda 45 spectrophotometer at 200–400 nm using quartz cells of 1 cm. The intrinsic and synchronous fluorescence spectra were recorded on a Hitachi F 7000 spectrofluorometer. The excitation and emission slit widths were adjusted to 5 nm with a PMT voltage of 500 V. The intrinsic fluorescence measurements were performed at excitation wavelengths of 280 and 295 nm, whereas the synchronous fluorescence spectrophotometric measurements were performed at $\Delta\lambda$ ($\lambda_{em} - \lambda_{ex}$) = 15 and 60 nm. Moreover, the circular dichroism (CD) spectrophotometric recordings were obtained with a Jasco J-815 spectropolarimeter using a quartz cuvette of 0.2 nm. The geometry of ceftazidime was optimized at DFT/B3LYP/6-31 using the ORCA program [22], and the analysis and visualization were performed using the Avogadro software [23]. The methodology applied for the molecular docking studies of the ceftazidime complex with BSA is described in the supplementary section.

3. Results and discussion

3.1. UV–Vis spectroscopy

The UV–Vis absorption spectrum of ceftazidime in 20 mM Tris-HCl buffer (pH 7.4) (Fig. 1A), that of BSA in the absence and presence of ceftazidime (Fig. S1), and the difference UV–Vis spectra after subtracting the contribution of ceftazidime from the BSA–ceftazidime complex (Fig. 1B) were recorded. Two characteristic peaks of cephalosporin antibiotics at around 230 and 260 nm could be observed (Fig. 1A), which corresponded to n → π* and π → π* transitions, respectively [24,25]. Moreover, two characteristic peaks of BSA were also detected in Fig. 1B, i.e., a strong peak at around 220 nm [26], which corresponds to the entire polypeptide chain and indicates its secondary structure, and a weak peak at 280 nm due to the absorption of aromatic amino acid residues, including tryptophan, tyrosine, and phenylalanine [27]. Thus, the UV–Vis absorption spectrum of BSA in the range of 200–400 nm can provide information about the secondary and tertiary structural changes in the protein [27]. It is clear from Fig. 1B that the absorbance of the peak corresponding to the polypeptide chain peak decreased as the ceftazidime concentration increased from 10 to 30 μM, indicating its effect on the secondary structure of BSA. Furthermore, a hypochromic shift at 280 nm in the presence of the drug was also ascribed to the formation of the ceftazidime–BSA complex.

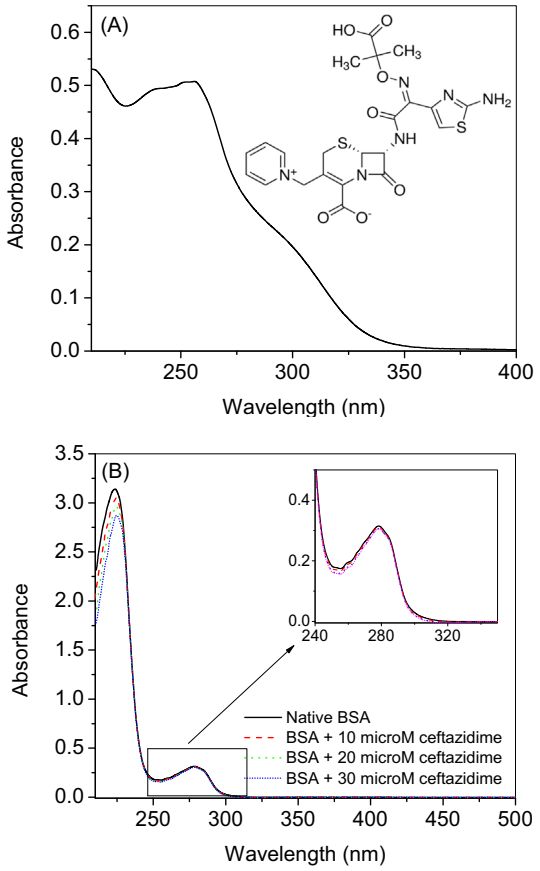

Fig. 1. (A) UV–Vis spectrum of 25 μM ceftazidime in 20 mM Tris-HCl buffer (pH 7.4). (B) Difference UV–Vis spectra of BSA (7 μM) in the absence and presence of various ceftazidime concentrations.

3.2. Fluorescence spectroscopy

BSA is a large heart-shaped protein with 583 amino acids divided into three functional domains (I, II, and III) and each of them is further sub-divided into two sub-domains (A and B). Two tryptophan residues, Trp134 and Trp213, are located in the sub-domains IB and IIA, respectively, and several tyrosine residues are distributed throughout the protein backbone [11,28]. Among the various amino acid residues in BSA, the aromatic tryptophan, tyrosine, and phenylalanine exhibit fluorescence emission when excited at certain wavelengths. The maximum fluorescence emission of BSA is attributed to the tryptophan residues, followed by a small contribution of tyrosine, while phenylalanine has a negligible contribution [11,29,30]. The protein excitation at 280 nm results in the fluorescence emission of both the tryptophan and tyrosine residues, while the excitation at 295 nm leads only to the tryptophan emission [30]. Considering these properties of BSA, its intrinsic fluorescence can be exploited to identify its structural changes when it binds to small molecules, especially drugs. Thus, in this study, the intrinsic fluorescence of BSA was studied at both excitation wavelengths (280 and 295 nm) to (i) determine the contribution of the tyrosine residue to the binding and (ii) to elucidate the extent and mechanism of the binding. According to the fluorescence emission spectra of BSA recorded in the presence of various ceftazidime concentrations at 280 and 295 nm (Fig. 2A and B, respectively), the maximum emission was observed at around 340 nm. It should also be noted that ceftazidime exhibited a significant absorption at both excitation wavelengths and in the most

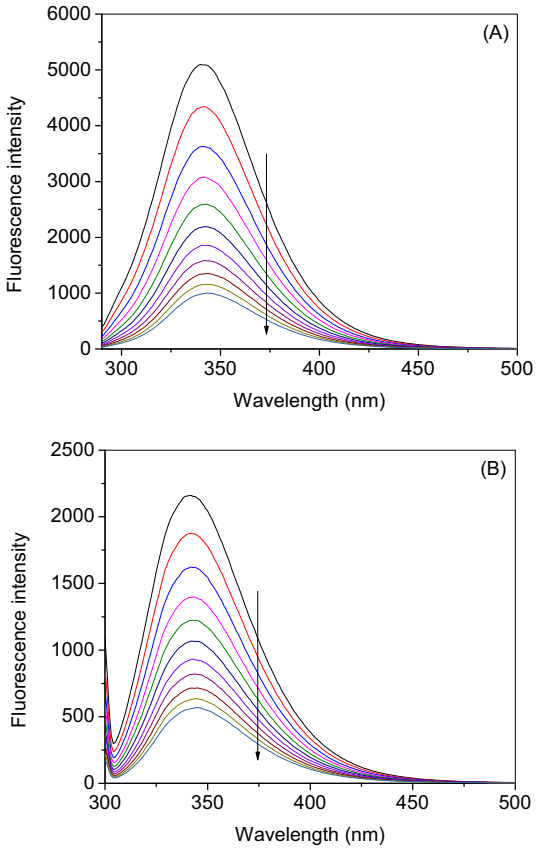

Fig. 2. Fluorescence emission spectra of BSA (3 μM) in the presence of various ceftazidime concentrations (0, 10, 20, 30, 40, 50, 60, 70, 80, 90, and 100 μM) at (A) $\lambda_{ex} = 280$ nm and (B) $\lambda_{ex} = 295$ nm at 25 °C in 20 mM Tris-HCl buffer (pH 7.4).

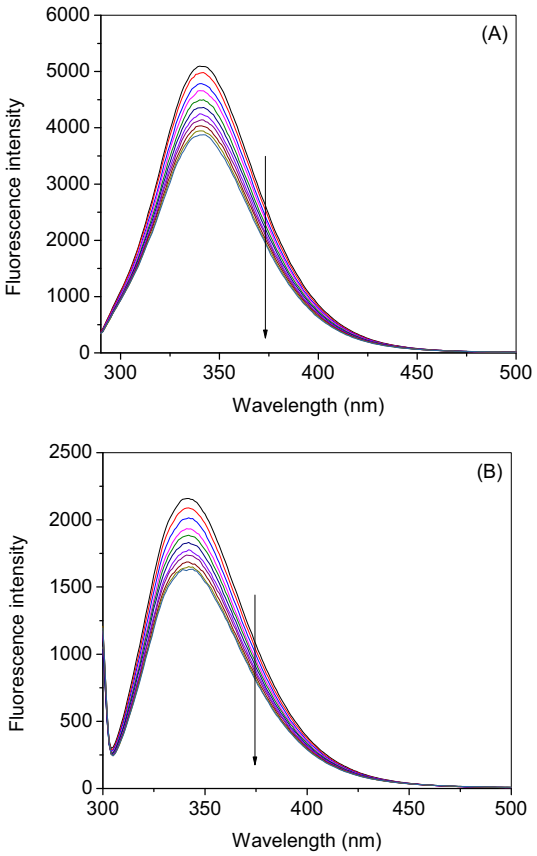

Fig. 3. Corrected fluorescence emission spectra of BSA (3 μM) in the presence of various ceftazidime concentrations (0, 10, 20, 30, 40, 50, 60, 70, 80, 90, and 100 μM) at (A) $\lambda_{ex} = 280$ nm and (B) $\lambda_{ex} = 295$ nm at 25 °C in 20 mM Tris-HCl buffer (pH 7.4).

significant emission range, indicating that the correction of the inner filter effect is essential. Thus, the inner filter effect for all the fluorescence emission spectra was corrected using the following equation [30]:

$$F_{corr} = F_{obs} \times 10^{(A_{exi}+A_{emi})/2} \quad (1)$$

where F_{corr} and F_{obs} are the corrected and observed fluorescence emission intensities of BSA, respectively, and A_{exi} and A_{emi} represent the absorbance of ceftazidime at the excitation and emission wavelengths, respectively. The corrected fluorescence spectra at 280 and 295 nm were then plotted (Fig. 3A and B), while the change in the relative fluorescence intensities (RFIs) obtained from the corrected fluorescence data at 340 nm with increasing ceftazidime concentration was also observed for both excitation wavelengths (Fig. 4). Although a difference could be observed in the RFIs obtained from the uncorrected data at 280 and 295 nm (Fig. S2), the difference between the RFIs of the corrected fluorescence data was insignificant, suggesting that the contribution of tyrosine in the interaction was very low [31,32]. Thus, due to this minor difference between the corrected RFIs at both wavelengths, the data obtained after excitation at 295 nm were used for further analysis.

Fluorescence is defined as the emission of light when a fluorophore absorbs light from a source. Any substance that can reduce the fluorescence of a fluorophore is known as a quencher and the relative process is known as quenching, which includes various molecular interactions such as ground-state complex formation, collisional quenching, and energy transfer [30]. Generally, these molecular interactions take place either by static quenching, where a stable fluorophore–quencher complex is formed, or by dynamic quenching due to the collisional encounters between the fluorophore and the quencher. The static and dynamic quenching can be differentiated by adjusting the temperature, as static quenching decreases with temperature increase, whereas dynamic quenching increases under the same conditions. Furthermore, since dynamic quenching is associated with a lower bimolecular quenching constant (K_q) of approximately 1×10^{10} M^{-1} s^{-1}, the diffusion-controlled limit and its higher value is connected with static quenching [30]. To understand the quenching type involved in the BSA–ceftazidime interaction, the studies were performed at two additional temperatures (35 °C and 45 °C) and their respective observed

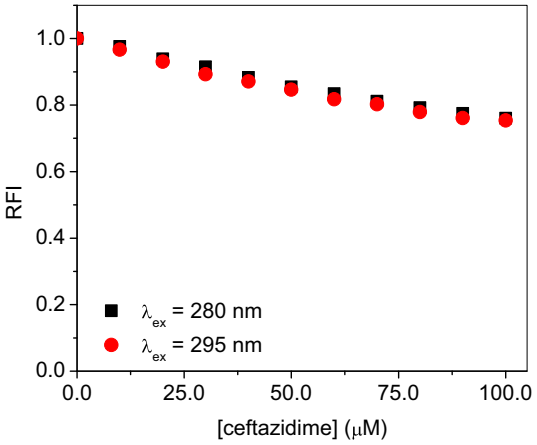

Fig. 4. Change in the RFIs of the BSA fluorescence emission at $\lambda_{ex} = 280$ and 295 nm with increasing ceftazidime concentration at 25 °C after correcting the inner filter effect.

and corrected fluorescence spectra were recorded (Figs. S3–S6). In general, the quenching of a fluorophore's fluorescence can be analyzed using the Stern–Volmer equation [30,33]:

$$\frac{F_0}{F} = 1 + K_{SV}[Q] \quad (2)$$

where F_0 and F indicate the emission intensity of BSA in the absence and presence of ceftazidime, respectively, K_{SV} is the Stern–Volmer constant, and [Q] is the concentration of the quencher [33]. Moreover, the K_{SV} factor is related to K_q according to the following relation:

$$K_q = \frac{K_{SV}}{\tau_0} \quad (3)$$

where τ_0 indicates the fluorophore's average lifetime in the absence of the quencher and has a value of 5.9×10^{-9} s^{-1} [34]. Herein, the K_{SV} values were obtained from the plots of F_0/F versus [Q] obtained with intercept = 1 at various temperatures (Fig. 5, Table 1). The calculated values were then used to estimate the K_q factor using Eq. (3). As observed in Table 1, the decrease in K_{SV} with increasing temperature and the significantly high value of K_q compared to the diffusion-controlled limit suggested that the interactions between BSA and ceftazidime were developed by static quenching.

Furthermore, the Stern–Volmer equation can be modified as follows to calculate the binding constant (K_b) and the number of binding sites (n) [35]:

$$log\frac{F_0 - F}{F} = logK_b + nlog[Q] \quad (4)$$

The K_b values (Table 2) obtained by the linear regression of Eq. (4) and the plots in Fig. 6 at 25 °C, 35 °C, and 45 °C were then used to calculate the thermodynamic parameters with the van't Hoff equation (Eqs. S1 and S2, Fig. 7A). A strong 1:1 binding between ceftazidime and BSA was identified, while the K_b values were in the 10^3 order of magnitude (Table 2). Moreover, the binding free energies (ΔG) indicated that the binding between BSA and ceftazidime was a spontaneous process, while the positive ΔH and ΔS values suggested that the binding was an endothermic process with increased disorderness.

Furthermore, the thermodynamic parameters can be used to clarify the type of forces involved in the interactions between proteins and small molecules, as sufficiently reported by Ross and Subramanian [36]. In particular, positive ΔH and ΔS values are generally attributed to hydrophobic interactions, whereas negative values are related to hydrogen bonding forces. In addition, if the ΔH value is close to the zero and ΔS is positive, the binding involves ionic interactions. Therefore, the positive ΔH and ΔS values observed in this study implied that hydrophobic interactions predominated. However, other forces, such as hydrogen bonding, van der Waals, and ionic interactions, cannot be excluded [37,38].

Table 1
Analyzed values of the quenching parameters of the BSA–ceftazidime interaction.

T (K)	K_{sv} (M^{-1})	K_q (M^{-1} s^{-1})	R^2
293	3.5×10^3	6.0×10^{11}	0.9911
303	3.4×10^3	5.9×10^{11}	0.9936
310	3.2×10^3	5.4×10^{11}	0.9971

Table 2
Binding and thermodynamic parameters of the BSA–ceftazidime interaction.

T (K)	n	K_b (M^{-1})	R^2	ΔG (KJ mol^{-1})	ΔH (KJ mol^{-1})	ΔS (J mol^{-1} K^{-1})
293	1.0	2.8×10^3	0.9947	−20.6	43.3	212.3
303	1.0	7.0×10^3	0.9934	−22.1		
310	1.0	8.2×10^3	0.9902	−24.2		

In order to check the involvement of hydrophobic interactions in the binding of ceftazidime and BSA, 8-anilino-1-naphthalenesulfonic acid (ANS) was used as an extrinsic fluorescence dye to. ANS, when excited at 380 nm in the presence of proteins, shows a large increase in fluorescence with a blue shift at the maximum emission compared to its fluorescence in an aqueous buffered solution [39], due to its binding with the hydrophobic protein patches. Thus, a compound that interacts with proteins via hydrophobic interactions may compete and displace the already bound ANS, thus decreasing the fluorescence emission of ANS [40–42]. As observed in the fluorescence spectrum of the BSA–ANS complex (Fig. 7B), the fluorescence intensity of ANS decreased with the successive addition of ceftazidime, indicating the competition of the two compounds for binding to the hydrophobic protein patches.

Synchronous fluorescence spectroscopy was also used to study the changes in the specific microenvironments near the tyrosine and tryptophan residues. The tyrosine and tryptophan emissions can be separated by simultaneously changing the excitation and emission wavelengths at $\Delta\lambda = 15$ and 60 nm, respectively [43]. The observed synchronous fluorescence spectra of BSA with various concentrations of ceftazidime are presented in Fig. S7 and the spectra obtained after the correction of the inner filter effect are depicted in Fig. 7C. Based on these results, tyrosine, emitting only at $\Delta\lambda = 15$ nm had a negligible contribution in the fluorescence quenching compared to tryptophan ($\Delta\lambda = 60$ nm), suggesting that no significant change occurred in the microenvironment of tyrosine in contrast to tryptophan. Moreover, the

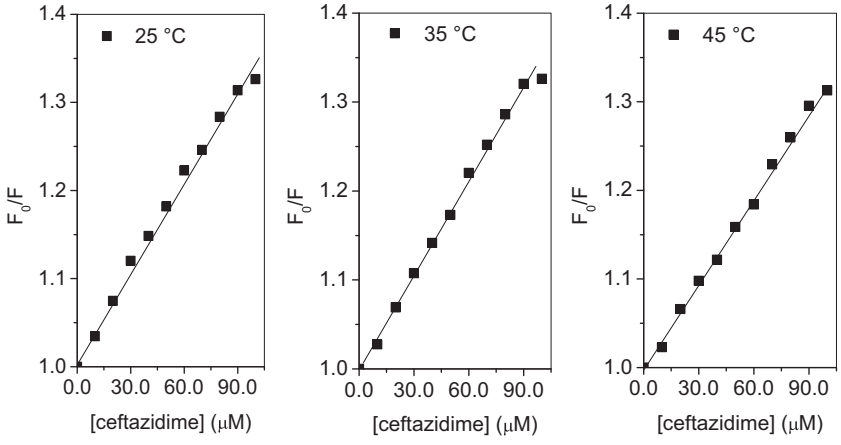

Fig. 5. Stern–Volmer plots of the BSA and ceftazidime interactions at various temperatures.

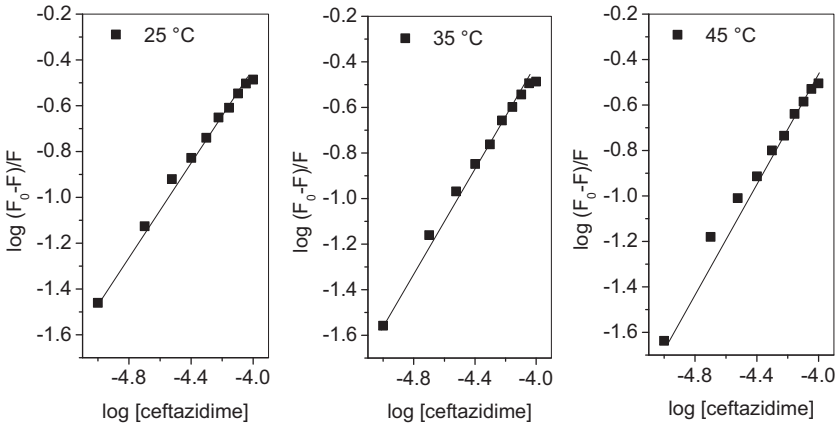

Fig. 6. Plots of log $(F_0 - F)/F$ versus log[ceftazidime] of the BSA and ceftazidime interactions at various temperatures.

results were consistent with those obtained from the fluorescence quenching experiments at 280 and 295 nm.

The Förster resonance energy transfer (FRET) theory is also important for understanding protein–ligand bindings, as it can describe the efficient energy transfer from the fluorophore of a protein to a ligand, provided that (i) the fluorescence spectrum of the protein and the absorption spectrum of the ligand overlap, (ii) their dipoles are close enough, and (iii) the distance between them is <8 nm [44]. Based on this theory, the energy transfer efficiency (E) can be calculated as follows:

$$E = 1 - \frac{F}{F_0} = \frac{R_0^6}{R_0^6 + r^6} \tag{5}$$

where r represents the distance between ceftazidime and BSA, and R_0 is the critical distance, which can be calculated by Eq. (6) when the transfer efficiency is 50%:

$$R_0^6 = 8.8 \times 10^{-25} k^2 N^{-4} \Phi J \tag{6}$$

where N is the refractive index of the medium, k^2 is the orientation factor, and Φ is the quantum yield of BSA. In addition, the spectral overlap integral (J) between the BSA emission spectrum and the absorbance spectrum of ceftazidime can be estimated as follows:

$$J = \frac{\sum F(\lambda)\varepsilon(\lambda)\lambda^4 \Delta\lambda}{\sum F(\lambda)\Delta\lambda} \tag{7}$$

where $F(\lambda)$ is the fluorescence intensity of BSA, $\varepsilon(\lambda)$ is the molar extinction coefficient of ceftazidime, and the values of k^2, N, and Φ are set to 2/3, 1.336, and 0.15, respectively [45]. The corresponding overlap of the ceftazidime UV–Vis spectrum and the fluorescence spectrum of BSA is depicted in Fig. 7D. Moreover, the E, and R_0 values were found to be 0.112 and 1.64 nm respectively, while r (2.24 nm) was <8 nm and $0.5R_0 < r < 1.5R_0$, indicating the energy transfer from BSA to ceftazidime.

3.3. Circular dichroism spectroscopy

It has been earlier reported that BSA has around 60% α-helicity [11,29] and exhibits negative CD bands at 208 and 222 nm due to $n \rightarrow \pi^*$ transitions, as depicted in Fig. 7E. In the presence of 20 μM ceftazidime the negative CD signal of BSA was reduced and further decreased as the drug concentration increased to 50 μM. Moreover, the α-helical composition of BSA was found to be 60.2% for native BSA using Eqs. (S3) and (S4), which was very close to the already reported value [11]. The equimolar concentration of ceftazidime had a negligible effect on the far-UV CD spectrum of native BSA (the plot is not included due to overlap), but the α-helicity in the presence of 20 μM and 50 μM decreased to 56.6% and 53.3%, respectively. Given that the bound drug destroys the hydrogen bonding network of the polypeptide chain and unfolds the protein by interacting with the amino acids [46], the decrease in the α-helicity indicated the partial unfolding of BSA by ceftazidime.

3.4. Molecular docking studies

Apart from various biophysical studies, molecular docking is an essential computational tool for understanding the interaction mechanisms of ligand molecules with target proteins through the analysis of various structural parameters such as binding orientation or docking poses, binding mode, the type of intermolecular interactions, key interacting residues of the target protein, estimated ΔG, estimated inhibition constant (K_i), etc. In this study, a molecular docking approach was developed to elucidate the interaction mechanism of the drug with the binding pocket of BSA, indicating that ceftazidime exhibited significant binding affinity ($\Delta G = -8.65$ kcal/mol and $K_i = 453.19$ nM) to the binding site of BSA. Three functional domains (domain 1:1–190, domain 2:191–382, and domain 3:383–583) were identified along with numerous binding sites responsible for binding to fatty acids, drug molecules, and bilirubin. Furthermore, ceftazidime occupied mainly the interface between the BSA domains 1 and 3, while few residues of domain 2 also participated.

Although the molecular docking study mainly focused on the predominance of the hydrophobic interactions in the binding, several types of intermolecular interactions (conventional hydrogen bonds, non-conventional hydrogen bonds, van der Waals, π-sulfur, and hydrophobic interactions) were also observed between the protein and the drug molecules. Moreover, most of the residues were located in the BSA domains 1 and 3, while those that formed van der Waals interactions with the drug were Ser109, Pro110, Asp111, Leu112, Pro113, Lys114, Leu115, Pro146, Arg185, Leu189, Thr190, Arg196, Glu424, Asn457, and Tyr451. In addition, the domain 1 of BSA was mainly involved in the van der Waals interactions with the drug molecule, while few residues from domains 2 and 3 participated. Asp108, Arg144, Ser192, and Arg458 formed classical hydrogen bonding interactions with ceftazidime, whereas the Ser109 and His145 residues participated in non-classical hydrogen bonding (C—H bonding) interactions. Moreover, three residues (Ala193, Leu454, and Ile455) developed π-alkyl interactions, while the His145 residue developed π-sulfur interactions with the drug molecule. For the validation, reliability, and reproducibility of the results, three different docking programs were employed and the results were analyzed based on a consensus approach. In particular, three programs were used to study the

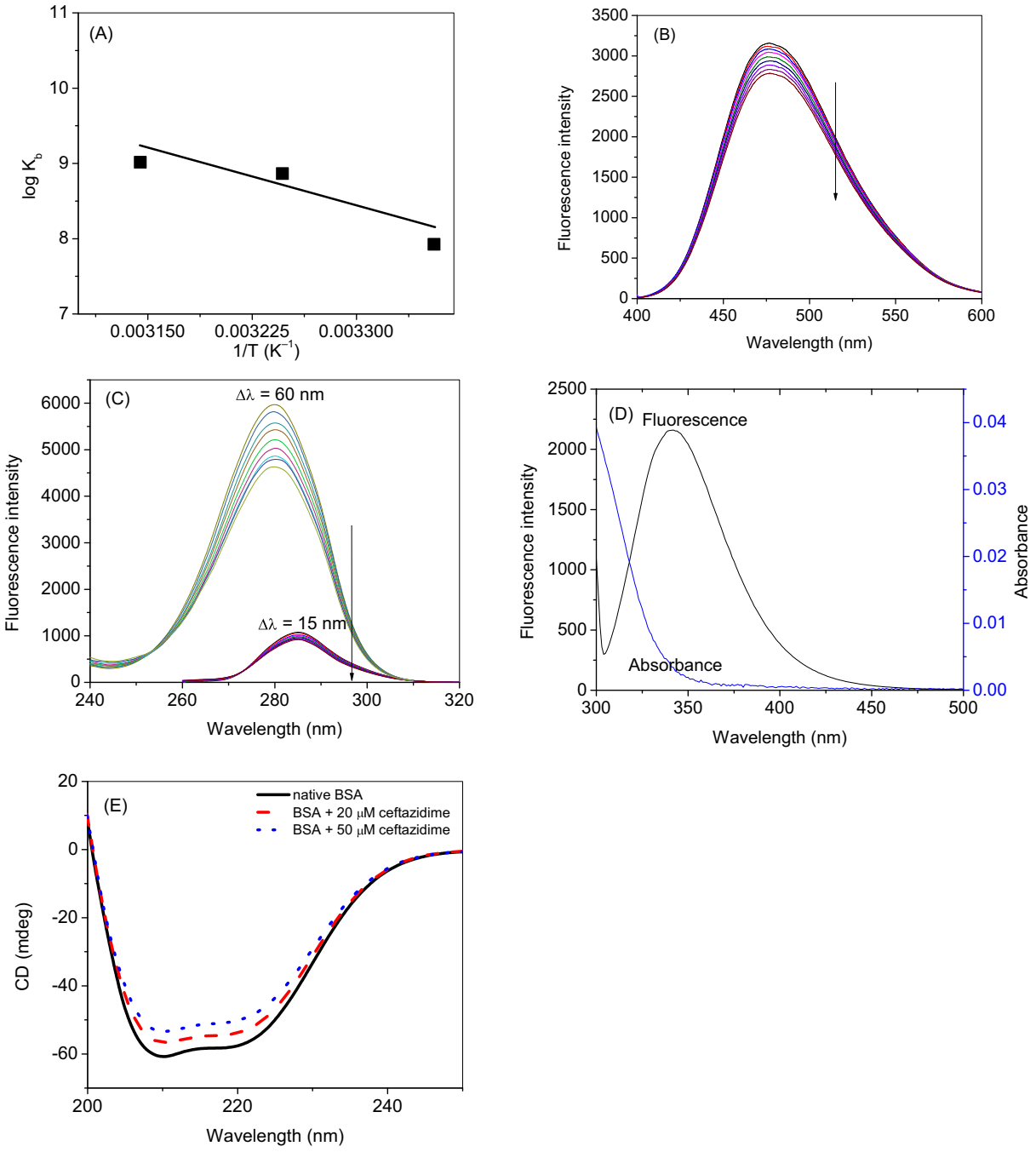

Fig. 7. (A) van't Hoff plot of the BSA interaction with ceftazidime; (B) Fluorescence spectra of the BSA (3 μM)–ANS (10 μM) complex in the presence of various ceftazidime concentrations (0, 10, 20, 30, 40, 50, 60, 70, and 80 μM) at 25 °C in 20 mM Tris-HCl buffer (pH 7.4). (C) Corrected synchronous fluorescence spectra of BSA (3 μM) in the presence of various ceftazidime concentrations (0, 10, 20, 30, 40, 50, 60, 70, and 80 μM) at 25 °C in 20 mM Tris-HCl buffer (pH 7.4). (D) Overlap of the fluorescence spectrum of BSA (3 μM) and the UV–Vis spectrum of ceftazidime (10 μM). (E) Far-UV CD spectra of BSA in the absence and presence of ceftazidime.

interactions of ceftazidime with BSA, namely AutoDock [47], AutoDock Vina [48] and PatchDock [49] (supplementary file). Interestingly, the results obtained from the three programs were consistent and were oriented in the interface of two BSA domains. More specifically, it was suggested that the drug molecule was mainly located in the interface between the BSA domains 1 and 3, while few residues of domain 2 also participated. The details of the interfacial residues between BSA and ceftazidime were also identified (Table 3). Furthermore, the interactions estimated from molecular docking were consistent with the interfacial statistics obtained from the PRODIGY server [50]. Therefore, based on the interfacial analysis results, the drug molecule was mainly oriented in domains 1 and 3 and partially in domain 2. The contribution percentage of each domain's residues to the drug molecule was estimated as follows: domain 1 = 51% (total number of interfacial residues 23/45), domain 2 = 33% (total number of interfacial residues 7/45), and domain 3 = 16% (total number of interfacial residues 15/45). The overall results indicated that the drug molecules mainly interacted with the BSA domain 1, while few residues of domains 2 and 3 contributed to the interactions.

The role of the ceftazidime flexibility in the binding due to its ten rotatable bonds was also explored. Therefore, the spatial arrangement of the atoms, bond lengths, and bond angles of free ceftazidime in the

Table 3
Interfacial residues between the three domains of BSA and ceftazidime.

Domain 1	Domain 2	Domain 3
Gln29	Ser191	Pro420
Gln32	Ser192	Thr421
Lys106	Ala193	Val423
Asp107	Arg194	Glu424
Asp108	Arg196	Val425
Ser109	Gln195	Arg427
Pro110	Leu197	Ser428
Asp111		Lys431
Leu112		Leu454
Glu140		Ile455
Ile141		Asn457
Ala142		Arg458
Arg143		Leu459
Arg144		Val461
His145		Leu462
Pro146		
Tyr147		
Phe148		
Arg185		
Glu186		
Val188		
Leu189		
Thr190		

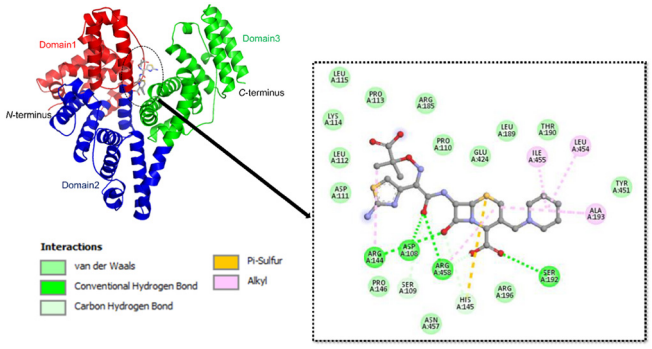

Fig. 8. Binding orientation of ceftazidime to BSA (left) and schematic representation of the BSA–ceftazidime intermolecular interactions (right). The figures were prepared by PyMOL and Discovery Studio, respectively.

gas state was compared with that in the BSA–ceftazidime complex with the lowest binding free energy obtained by the molecular docking studies (Fig. 8). A remarkable change was observed in the geometry of ceftazidime after its binding to BSA, indicating that ceftazidime adopted the environment of the BSA binding site to develop stronger interactions and form a stable complex [51].

3.5. DFT studies

The frontier molecular orbitals (FMOs) (highest occupied molecular orbital (HOMO) and lowest unoccupied molecular orbital (LUMO)) of free ceftazidime and its complex with BSA (Fig. 9), were also evaluated using the density functional theory (DFT) method. The HOMOs of free ceftazidime were detected in the pyridinium-1-ylmethyl group, which was located at the 3-position of the antibiotic's cephem ring. However, when the BSA–ceftazidime complex was formed, the HOMOs shifted to the central cephem ring. In contrast, the position of LUMOs remained almost unchanged for free and complexed ceftazidime, but a change could be observed in their relative sizes. The energy gap between HOMO and LUMO was calculated using the formula:

$$\Delta E = E_{LUMO} - E_{HOMO} \tag{8}$$

The energy associated with HOMO and LUMO was then used to calculate the chemical potential (μ) and chemical hardness (η) of the system:

$$\mu = \frac{E_{LUMO} + E_{HOMO}}{2} \tag{9}$$

$$\eta = \frac{E_{LUMO} - E_{HOMO}}{2} \tag{10}$$

Generally, the ionization potential (I) is defined as the $-E_{HOMO}$ value, while the electron affinity (A) is equal to $-E_{LUMO}$. Thus, the electronegativity (χ) and electrophilicity (ω) can be calculated according to the following equations:

$$\chi = \frac{I + A}{2} \tag{11}$$

$$\omega = \frac{\mu^2}{2\eta} \tag{12}$$

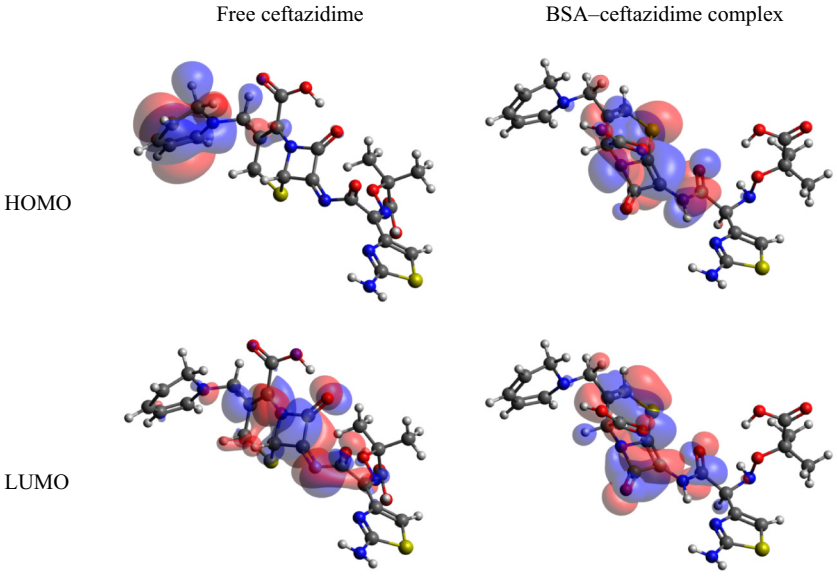

Fig. 9. FMO diagrams of free ceftazidime and after the BSA–ceftazidime complex obtained through the geometry optimization.

Table 4
Various quantum chemical parameters obtained by DFT calculations. The energy unit is eV.

	Free ceftazidime	BSA–ceftazidime complex
HOMO	−4.945	−5.342
LUMO	−3.114	−1.583
Energy gap (ΔE)	1.831	3.759
Chemical potential (μ)	−4.0295	−3.4625
Global hardness (η)	0.9155	1.8795
Ionization potential ($I = -E_{HOMO}$)	4.945	5.342
Electron affinity ($A = -E_{LUMO}$)	3.114	1.583
Electronegativity [($\chi = (I + A)/2$)]	4.0295	3.4625
Electrophilicity [($\omega = \mu^2/2\eta$)]	8.8678	3.1894

Based on the data of the DFT calculations (Table 4), the energy gap between the HOMO and LUMO of complexed ceftazidime was significantly higher than that of the free drug. Generally, a molecule with a small frontier orbital gap is more polarizable and has high chemical reactivity and low kinetic stability [52], whereas a larger gap leads to a greater molecular stability for further reactions [53]. Herein, the large gap in the energies of HOMO and LUMO was attributed to the stability of the molecule, which was in turn due to the formation of the stable BSA–ceftazidime complex. Moreover, the chemical hardness (η) of a system is defined as the resistance to deformation of the electron cloud of chemical systems under disturbance encountered during a chemical process and is parallel to the stability of a molecule [54,55]. The η value of the BSA–ceftazidime complex was higher than that of the free drug, suggesting the greater stability of the complex and the interaction between BSA and ceftazidime.

4. Conclusions

The interaction of ceftazidime with BSA was studied using experimental and computational methods. A 1:1 reasonable interaction was identified, which occurred through a static quenching mechanism and mainly facilitated by hydrophobic, hydrogen bonding, and van der Waals forces. Moreover, ceftazidime was located in the interfacial region of the three BSA domains and its stability was increased in the binding cavity of BSA. Among them, the domain 1 contributed the maximum to the binding. In addition, BSA was partially unfolded in the presence of ceftazidime. However, the geometry of BSA-complexed ceftazidime was significantly changed compared to the free drug due to its interaction with amino acids and its adjustment in the binding pocket. The FMOs of free and complexed ceftazidime were also calculated using the DFT method. According to the values of chemical hardness and the energy gap between the HOMOs and LUMOs, the complexed ceftazidime was more stable, complying with the experimental results and the feasibility of the interaction.

CRediT authorship contribution statement

Mohd. Sajid Ali: Investigation, Formal analysis, Writing - original draft, Writing - review & editing,**Jayaraman Muthukumaran:**Investigation, Writing - original draft, Writing - review & editing.**Hamad A. Al-Lohedan:**Writing - original draft, Writing - review & editing.

Declaration of competing interest

The authors declare no conflict of interests.

Acknowledgements

The authors (MSA and HAA) are grateful to the Deanship of Scientific Research, King Saud University for funding through Vice Deanship of Scientific Research Chairs. The authors thank the Deanship of Scientific Research and RSSU at King Saud University for their technical support.

Appendix A. Supplementary data

Supplementary data to this article can be found online at https://doi.org/10.1016/j.molliq.2020.113490.

References

[1] R.I. Aminov, A brief history of the antibiotic era: lessons learned and challenges for the future, Front. Microbiol. 1 (2010).
[2] K. Gould, Antibiotics: from prehistory to the present day, J. Antimicrob. Chemother. 71 (2016) 572–575.
[3] K.C. Nicolaou, S. Rigol, A brief history of antibiotics and select advances in their synthesis, J. Antibiot. 71 (2018) 153–184.
[4] W.F. Marshall, J.E. Blair, The cephalosporins, Mayo Clin. Proc. 74 (1999) 187–195.
[5] World Health Organization Model List of Essential Medicines, 21st List. , World Health Organization, Geneva, 2019 (Licence: CC BY-NC-SA 3.0 IGO).
[6] M.G. Papich, Ceftazidime, in: M.G. Papich (Ed.), Saunders Handbook of Veterinary Drugs (Fourth Edition), W.B. Saunders, St. Louis 2016, pp. 135–136.
[7] D.M. Richards, R.N. Brogden, Ceftazidime - a review of its antibacterial activity, pharmacokinetic properties and therapeutic use, Drugs 29 (1985) 105–161.
[8] A. Adu, C.L. Armour, Drug utilization review (Dur) of the 3rd-generation cephalosporins - focus on ceftriaxone, ceftazidime and cefotaxime, Drugs 50 (1995) 423–439.
[9] J.A. Colmer-Hamood, N. Dzvova, C. Kruczek, A.N. Hamood, In vitro analysis of Pseudomonas aeruginosa virulence using conditions that mimic the environment at specific infection sites, Prog. Mol. Biol. Transl. 142 (2016) 151–191.
[10] S. Schmidt, D. Gonzalez, H. Derendorf, Significance of protein binding in pharmacokinetics and pharmacodynamics, J. Pharm. Sci.-US 99 (2010) 1107–1122.
[11] J. Theodore Peters, All About Albumin: Biochemistry, Genetics, and Medical Applications, Academic Press, 1995.
[12] K.A. Bakar, S.D. Lam, H.M. Sidek, S.R. Feroz, Characterization of the interaction of diosgenin with human serum albumin and α1-acid glycoprotein using biophysical and bioinformatic tools, J. Mol. Liq. 306 (2020), 112865. .
[13] F. Fathi, M. Sharifi, A. Jafari, N. Kakavandi, S. Kashanian, J. Ezzati Nazhad Dolatabadi, M.-R. Rashidi, Kinetic and thermodynamic insights into interaction of albumin with piperacillin: spectroscopic and molecular modeling approaches, J. Mol. Liq. 296 (2019), 111770. .
[14] Q. Zhang, Z. Zhu, Y. Ni, Interaction between aspirin and vitamin C with human serum albumin as binary and ternary systems, Spectrochim. Acta A Mol. Biomol. Spectrosc. 236 (2020), 118356. .
[15] S. Zargar, S. Alamery, A.H. Bakheit, T.A. Wani, Poziotinib and bovine serum albumin binding characterization and influence of quercetin, rutin, naringenin and sinapic acid on their binding interaction, Spectrochim. Acta A Mol. Biomol. Spectrosc. 235 (2020), 118335. .
[16] M.K. Siddiqi, P. Alam, S.K. Chaturvedi, S. Nusrat, M.R. Ajmal, A.S. Abdelhameed, R.H. Khan, Probing the interaction of cephalosporin antibiotic-ceftazidime with human serum albumin: a biophysical investigation, Int. J. Biol. Macromol. 105 (2017) 292–299.
[17] B. Nerli, D. Romanini, G. Pico, Structural specificity requirements in the binding of beta lactam antibiotics to human serum albumin, Chem. Biol. Interact. 104 (1997) 179–202.
[18] C.-X. Huo, L. Bai, J.J. Ren, Interaction between ceftazidime and bovine serum albumin found by spectroscopy, J. Gansu Sci. 20 (2008) 60–63.
[19] M.S. Ali, H.A. Al-Lohedan, Spectroscopic and computational evaluation on the binding of safranal with human serum albumin: role of inner filter effect in fluorescence spectral correction, Spectrochim. Acta A 203 (2018) 434–442.
[20] M.S. Ali, H.A. Al-Lohedan, Experimental and computational investigation on the molecular interactions of safranal with bovine serum albumin: binding and anti-amyloidogenic efficacy of ligand, J. Mol. Liq. 278 (2019) 385–393.
[21] M.S. Ali, H.A. Al-Lohedan, Spectroscopic and molecular docking investigation on the noncovalent interaction of lysozyme with saffron constituent "Safranal", ACS Omega 5 (2020) 9131–9141.
[22] F. Neese, Software update: the ORCA program system, version 4.0, Wires Comput. Mol. Sci. 8 (2018).
[23] M.D. Hanwell, D.E. Curtis, D.C. Lonie, T. Vandermeersch, E. Zurek, G.R. Hutchison, Avogadro: an advanced semantic chemical editor, visualization, and analysis platform, J Cheminformatics 4 (2012).
[24] D.B. Boyd, Electronic-structures of cephalosporin and penicillin moieties, J. Am. Chem. Soc. 94 (1972) 6513–6519.
[25] B. Vilanova, F. Munoz, J. Donoso, F. Garciablanco, Analysis of the UV absorption-band of cephalosporins, Appl. Spectrosc. 46 (1992) 44–48.
[26] H. Polet, J. Steinhardt, Binding-induced alterations in ultraviolet absorption of native serum albumin, Biochemistry 7 (1968) 1348–1356.
[27] B.A. Shirley, Protein Stability and Folding: Theory and Practice, Humana Press, 1995.
[28] D.C. Carter, J.X. Ho, Structure of serum-albumin, Adv. Protein Chem. 45 (1994) 153–203.
[29] R.J. Alekseev, A.L. Rebane, Serum Albumin: Structure, Functions, and Health Impact, Nova Science Publishers, 2012.
[30] J.R. Lakowicz, Principles of Fluorescence Spectroscopy, 3rd ed. Springer US, 2006.

[31] L. Trynda-Lemiesz, K. Wiglusz, Interactions of human serum albumin with meloxicam characterization of binding site, J. Pharm. Biomed. Anal. 52 (2010) 300–304.
[32] N. Ibrahim, H. Ibrahim, S. Kim, J.P. Nallet, F. Nepveu, Interactions between antimalarial indolone-N-oxide derivatives and human serum albumin, Biomacromolecules 11 (2010) 3341–3351.
[33] O. Stern, M. Volmer, Über die abklingzeit der fluoreszenz, Phys. Z. 20 (1919) 183–188.
[34] M.R. Eftink, Fluorescence quenching reactions, in: T.G. Dewey (Ed.), Biophysical and Biochemical Aspects of Fluorescence Spectroscopy, Springer US, Boston, MA 1991, pp. 1–41.
[35] M. Jiang, M.X. Xie, D. Zheng, Y. Liu, X.Y. Li, X. Chen, Spectroscopic studies on the interaction of cinnamic acid and its hydroxyl derivatives with human serum albumin, J. Mol. Struct. 692 (2004) 71–80.
[36] P.D. Ross, S. Subramanian, Thermodynamics of protein association reactions: forces contributing to stability, Biochemistry 20 (1981) 3096–3102.
[37] M.S. Ali, H.A. Al-Lohedan, Deciphering the interaction of procaine with bovine serum albumin and elucidation of binding site: a multi spectroscopic and molecular docking study, J. Mol. Liq. 236 (2017) 232–240.
[38] M.S. Ali, M. Amina, H.A. Al-Lohedan, N.M. Al Musayeib, Human serum albumin binding to the biologically active labdane diterpene "leoheterin": spectroscopic and in silico analysis, J. Photochem. Photobiol. B Biol..
[39] L. Brand, J.R. Gohlke, D.S. Rao, Evidence for binding of rose bengal and anilinonaphthalenesulfonates at active site regions of liver alcohol dehydrogenase, Biochemistry 6 (1967) 3510–3518.
[40] W. Du, T. Teng, C.C. Zhou, L. Xi, J.Z. Wang, Spectroscopic studies on the interaction of bovine serum albumin with ginkgolic acid: binding characteristics and structural analysis, J. Lumin. 132 (2012) 1207–1214.
[41] N. Zhou, Y.Z. Liang, P. Wang, Characterization of the interaction between furosemide and bovine serum albumin, J. Mol. Struct. 872 (2008) 190–196.
[42] N. Seedher, M. Kanojia, Reversible binding of antidiabetic drugs, repaglinide and gliclazide, with human serum albumin, Chem. Biol. Drug Des. 72 (2008) 290–296.
[43] J.B.F. Lloyd, Synchronized excitation of fluorescence emission spectra, Nat. Phys. Sci. 231 (1971) 64.
[44] T. Forster, in: O. Sinaoglu (Ed.), Modern Quantum Chemistry, Academic Press, New York, 1965.
[45] T. Forster, 10th spiers memorial lecture - transfer mechanisms of electronic excitation, Discuss Faraday Soc (1959) 7–17.
[46] J. Kang, Y. Liu, M.X. Xie, S. Li, M. Jiang, Y.D. Wang, Interactions of human serum albumin with chlorogenic acid and ferulic acid, Bba-Gen. Subject 1674 (2004) 205–214.
[47] G.M. Morris, R. Huey, A.J. Olson, Using AutoDock for ligand-receptor docking, current protocols in bioinformatics, chapter 8, Unit 8 (2008) 14.
[48] O. Trott, A.J. Olson, Software news and update AutoDock Vina: improving the speed and accuracy of docking with a new scoring function, efficient optimization, and multithreading, J. Comput. Chem. 31 (2010) 455–461.
[49] D. Schneidman-Duhovny, Y. Inbar, R. Nussinov, H.J. Wolfson, PatchDock and SymmDock: servers for rigid and symmetric docking, Nucleic Acids Res. 33 (2005) W363–W367.
[50] L.C. Xue, J.P.G.L.M. Rodrigues, P.L. Kastritis, A.M.J.J. Bonvin, A. Vangone, PRODIGY: a web server for predicting the binding affinity of protein-protein complexes, Bioinformatics 32 (2016) 3676–3678.
[51] B.-L. Wang, D.-Q. Pan, S.-B. Kou, Z.-Y. Lin, J.-H. Shi, Exploring the binding interaction between bovine serum albumin and perindopril as well as influence of metal ions using multi-spectroscopic, molecular docking and DFT calculation, Chem. Phys. (2019) 110641.
[52] D.F.V. Lewis, C. Ioannides, D.V. Parke, Interaction of a series of nitriles with the alcohol-inducible isoform of P450 - computer-analysis of structure-activity-relationships, Xenobiotica 24 (1994) 401–408.
[53] M.M. Lynam, M. Kuty, J. Damborsky, J. Koca, P. Adriaens, Molecular orbital calculations to describe microbial reductive dechlorination of polychlorinated dioxins, Environ. Toxicol. Chem. 17 (1998) 988–997.
[54] D. Sharma, H. Ojha, M. Pathak, B. Singh, N. Sharma, A. Singh, R. Kakkar, R.K. Sharma, Spectroscopic and molecular modelling studies of binding mechanism of metformin with bovine serum albumin, J. Mol. Struct. 1118 (2016) 267–274.
[55] Z.X. Zhou, R.G. Parr, Activation hardness - new index for describing the orientation of electrophilic aromatic-substitution, J. Am. Chem. Soc. 112 (1990) 5720–5724.